



Fluorescent nano particle application for a membrane surface integrity test: Sensitivity, stability, and reliability of the particles

Soo Hoon Choi^a, Juhee Yang^b, Byeong-Gyu Choi^c, Jinwoo Cho^{d,*}

^aDepartment of Civil and Environmental Engineering, University of Delaware, Newark, DE 19716, USA

^bKorea Institute of Construction & Transportation Technology Evaluation and Planning, 1600 Gwanyang-dong, Dongan-gu, Anyang-si, Gyeonggi-do 431-060, Republic of Korea

^cWater Resources Research Organization, Sejong University, 98 Gunja-Dong, Gwangjin-Gu, Seoul 143-747, Republic of Korea

^dDepartment of Environment & Energy, Sejong University, 98 Gunja-Dong, Gwangjin-Gu, Seoul 143-747, Republic of Korea

Tel. +82 2 3408 3970; Fax: +82 2 3408 4320; email: jinwoocho@sejong.ac.kr

Received 20 October 2010; Accepted 12 April 2012

ABSTRACT

In this research, silica-based fluorescent particles were synthesized and used as a surrogate detector to evaluate the integrity of a compromised flat sheet membrane. Three different sizes of particles were synthesized and dyed with a fluorescent dye to make a fluorescence image under a UV light. Experiments were designed to test the sensitivity of the detection limit, stability of particles, and reliability of the proposed method. UV spectrometer and image analysis were used to evaluate the detection limits and measure the concentration and mass of the particles in the feed and permeate. For the stability of the particles, dye-leakage tests were conducted to estimate the amount of fluorescent decay when fluorescent particles were dissolved in an aqueous solvent. The effect of the particles on the membrane fouling was also investigated by conducting a batch filtration test of undamaged membranes. To examine the reliability of the proposed method, a series of filtration tests were performed with the damaged membranes by applying the fluorescent particles as a surrogate. As a result, the image analysis could detect the maximum mass of particles of 5 mg. The particles showed the stable fluorescence intensity within 24 h after being dissolved into 100% ethanol solution. In considering the pore size in the membrane, the particles with a size of about three times larger than the membrane pores were the most compatible surrogate for the integrity test to prevent the undesirable affect of having the membrane fouling. Finally, the size of breach on the membrane surface could be predicted, possibly from the image analysis of the permeate containing the fluorescent particles outflow from a damaged part of the membrane surface.

Keywords: Fluorescent particle; Membrane; Integrity test; Fouling; Sensitivity

1. Introduction

Membrane filtration is being applied widely to the liquid–solid separation process in water treatment. In

general, a membrane tends to be damaged in its operation and have an opening hole or breach in the surface, and sometimes a crack in the frame [1]. The

*Corresponding author.

Membranes in Drinking and Industrial Water Treatment—MDIW 2010, June 27–30, 2010, Trondheim, Norway

1944-3994/1944-3986 © 2013 Balaban Desalination Publications. All rights reserved.

detection of these defective parts by the naked eye requires a very time-consuming and laborious process considering there are hundreds to thousands of membrane installations in use. To simplify the process, many direct or indirect integrity testing methods have been developed [2]. For the direct methods, pressure decay tests and the diffusive air flow tests are the most widely used methods [3,4]. These methods are of high sensitivities at up to 4.5–5 log removal of *Giardia* or *Cryptosporidium*, independent of feed water quality and without relying on filtered quality monitoring [5,6]. However, to carry out these methods, the membrane operation has to be interrupted, bringing production loss in the filtration process [7]. And also in some cases, the tests may cause additional membrane damage during the tests producing false-positive values [1]. On the other hand, indirect methods have been proposed. Particle and turbidity monitoring followed by various surrogate challenge tests are good examples of indirect methods. Indirect methods are convenient for routine qualitative monitoring and high feasibility of application in the field. However, in many cases, these methods result in lower detection sensitivity. To overcome that disadvantage, novel methods adapting new surrogates such as paramagnetic particles, gold nano-particles, and microbial particles have been proposed [2]. For paramagnetic tests, the particles are synthesized to flow through the compromised area to be later captured by a field. Magnetic sensors include a superconducting quantum interference device magnetometer, giant magneto-resistive sensors, measurement of magnetic permeability, and measurement of magnetic susceptibility. Laboratory-scale results of this method have been reported. On-line magnetic challenge tests for monitoring membrane integrity, with the advantages of detection specific, high detection sensitivity, and on-line operation, is a plausible one for large-scale applications [8,9]. However, real large-scale application in the field seems to be questionable due to the complexity of equipment and operation process. Gold nano-particles are preferred to other metal nano-particles due to the extremely low background level in a water system, non-pathogenicity, high monodispersity, and inexpensive price. Breaches in the membrane of diameters as small as 20 nm were detected with sensitivities as high as a level of part per billion. However, the anodic stripping voltammetry method for detecting the gold nano-particles needs a prolonged run time and the addition of another metal is required to solve this problem [10,11]. The microbial challenge test represents the degree of viral pathogen removal in membrane systems and has a good sensitivity to breaches in the membranes. However, the test is not effective for actual application in real treatment plants [12,13].

Choi et al. [15] recently proposed a novel method in which an optically functionalized silica particle is applied as a surrogate to check the integrity of microfiltration membranes. In this method, the outflow of the fluorescent particles through a damaged part was monitored in permeates under a UV lamp to obtain a fluorescence image. This image was then analyzed digitally to estimate the mass of outflow fluorescent particles and determine the size of the damaged area. The advantages of this method are to use an inexpensive surrogate based on silica and be able to measure quantitatively the size of a damaged part on a membrane surface. The principle of the method, testing process, and mathematical tools for predicting the size of a damaged part are well described in the reference in detail [15]. However, the previous study presents insufficient information on the sensitivity of the method such as a detection limit and the stability of the fluorescent particles, that is, the change of fluorescent intensity when dispersed in water solution over a long time. Additionally, the impact of surrogate particles on membrane fouling should be evaluated for the various sizes of particles to examine whether the surrogate may cause the unexpected fouling.

In this article, the sensitivity of the detection methods were evaluated by estimating the minimum and maximum detection limit of the method followed by a correlation between the particle amount and detection values. A dye-leakage test was conducted to evaluate the amount of fluorescent decay of particles when submerged in aqueous solutions for a long time. To evaluate the impact of the fluorescent particles on the membranes, fouling the cake formation and initial pore blocking by fluorescent particles were investigated. Finally, the membrane rejection rate of injected particles from punctured membranes was also measured for integrity test evaluation.

2. Materials and methods

2.1. Synthesis of silica-based fluorescent particle

Chemically modified silica particles were synthesized through the hydrolysis and condensation reactions via the Stöber process [14]. These silica particles were then functionalized by incorporating a covalently labeled fluorescent dye [16,17]. The procedure for the synthesis of the silica particles was as follows: 1.6 mL of hydrochloric acid (HCl, 0.1 M) was added to 80 mL of de-ionized water in a 100 mL Scott bottle, with continuous stirring. The pH of this solution was approximately 2.7. A 100 mL of 3-mercaptopropyltrimethoxysilane (MPTMS, 97%) was added to this acidified solution and stirred for 18 h.

The emulsion was separated by centrifugation at $3,000 \times g$ for 5 min. The collected supernatant was diluted with pH 3.5 de-ionized water to control the particle size. The concentration to which the supernatant had been diluted later determined the size of the synthesized particles, which produced smaller particles with a lower concentration of MPTMS. A $100 \mu\text{L}$ of triethylamine (TEA, 99%) was then rapidly added to this diluted solution. The development of silica particles was observed within 30 min after the addition of TEA. The solution-containing silica particles were then centrifuged at $3,000 \times g$ for 5 min. Finally, the separated particles were collected and washed with ethanol to remove any residual monomers and TEA. In this study, the supernatant was diluted into 1, 5, and 50% by volume base with de-ionized water to have three different particle sizes (208, 161, and 817 nm on average, respectively). A particle size analyzer (Zetasizer, Malvern) was used to measure the size of the particles. The synthesized silica particles were then dyed with rhodamine B isothiocyanate (RBITC), using the following procedure: RBITC solution ($1 \times 10^{-4}\text{M}$) was prepared in dimethylformamide (DMF). About $20 \mu\text{L}$ of RBITC solution was again diluted into $100 \mu\text{L}$ of DMF. This diluted RBITC solution was then added to the synthesized silica particles, and the mixture was stirred for 2 h in the dark. Finally, the products were washed with DMF and then ethanol to remove any residual RBITC. The synthesized fluorescent silica particles were stored in a brown-colored bottle at 4°C .

2.2. Membranes

All tested membranes were cut out from a flat sheet membrane (YUASA, Japan) to have a circular form with a diameter of 63.5 mm to fit the batch test instrument (Amicon cell™). The nominal pore size of the membrane is $0.25 \mu\text{m}$. All membranes were soaked in DI water for 24 h prior to the experiments.

2.3. Membrane filtration experiments

A batch test was performed with an Amicon cell™ to simulate a flat sheet membrane unit as depicted in Fig. 1. The cell consisted of an acrylic glass cylinder able to withstand an internal pressure of $0 \leq 5 \times 10^6 \text{ Pa}$ (50 bar). Feed solutions were pressurized with nitrogen gases throughout the tests, with a pressure regulator to control the pressure. An electronic scale was placed at the permeate end of the cell and connected to a computer to measure the permeate flow. Clean water flux experiments were conducted with solutions composed of DI water and ethanol of a ratio of 1:1 where

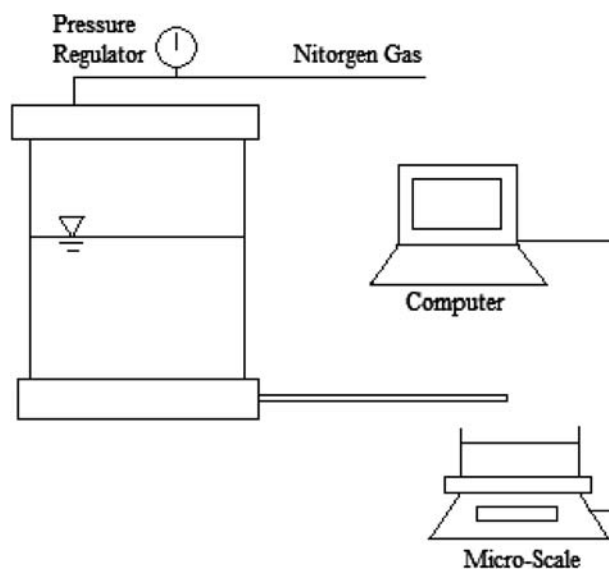


Fig. 1. Schematic of Amicon cell system.

the nano-particles were dispersed in the same solutions for maximum dispersion [18]. A micro-scale was connected to the permeate outflow to detect the flow rate from the intact cell, while the measured results were recorded to a computer automatically.

2.4. Image analysis of fluorescent particles

Image analysis was performed to convert the fluorescence intensity of silica particles into an RGB value (the red, green, and blue values of each pixel in the picture). A darkroom was constructed using a steel frame with dimension of $475 \times 340 \times 310 \text{ mm}$ ($L \times W \times H$) and a digital camera (Fuji FinePix s6000fd) was installed on top of the frame. Two 40 W UV lamps were placed inside the darkroom, at a distance of 120 mm, with an additional 4 W UV lamp placed perpendicular for even UV radiation.

After the filtration tests, membranes with particles deposition were dehydrated in a desiccator for 24 h and then placed between the UV lamps to be photographed by a digital camera. The photographs were taken under conditions of F/8, ISO-100 and an exposure time of 4 s. The pictures were then edited using Photoshop to eliminate the background and additional noises that may cause any misinterpretations of the pictures and stored in an RGB format (Fig. 2). The edited pictures were then quantified and calculated using the MATLAB. With this program, the red, green, and blue values of each pixel were added together and divided by the total number of pixels, showing the average RGB value. Since the image analysis emphasizes the fluorescent image of particles by removing the background image caused by the membranes and

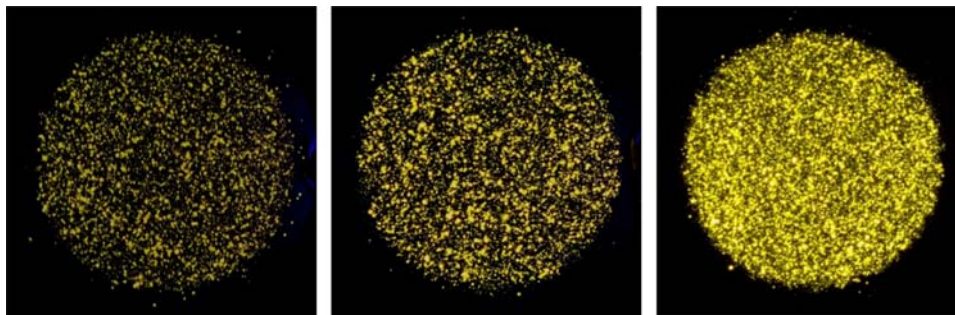


Fig. 2. Edited pictures for the image analysis (background noise removed graphically).

other noise signals, even a small extent of particles will be detected.

3. Results and discussion

3.1. Detection limit of fluorescent particles

As described previously, the image analysis produced the average RGB value for the fluorescence intensity of particles which were filtered through a 0.25 μm membrane. Also the mass of particles filtered was measured using a precise mass balance. The particle used in this experiment was made from 50% dilution (817 nm in average size). Fig. 3 shows the fluorescence intensity (RGB value) as a function of the filtered particle mass. The figure indicates that the fluorescence intensity increases almost linearly with the mass of particles up to about 3.0 mg of particle mass. Then, the increasing rate of intensity was decreased gradually from 3.0 to 5.0 mg of particle mass. There seemed to be no more increase and it

reached the maximum intensity after 5.0 mg of particle mass. Thus, as for the image analysis, the upper level of the detection limit on the particle mass was determined to be 5.0 mg.

The UV spectrometer (Beckman Coulter DU 730 Spectrophotometer) was used to measure the concentration of particles in an aqueous solution. We assumed UV absorbance may have a functional relationship with the concentration of dispersed fluorescent particles in the feed or permeate. Our previous experiment indicated that the fluorescent-particles show the highest absorbance under UV wavelengths of 550 nm. Under this UV wavelength, the absorbance of particles in aqueous solution was investigated with various particle concentrations ranging from 0.1 to 25 mg/L. Each concentration was measured three times to ensure the reproducibility of the result. As result, Fig. 4 shows the UV absorbance increases non-linearly with increase in particle concentration. In this case, as presented in Table 1, it should be noted that very unstable measurement of absorbance was observed at the low-concentration level of less than 5.0 mg/L. The measurement indicated that the minimum detective concentration of the particles is of 1.0 mg/L.

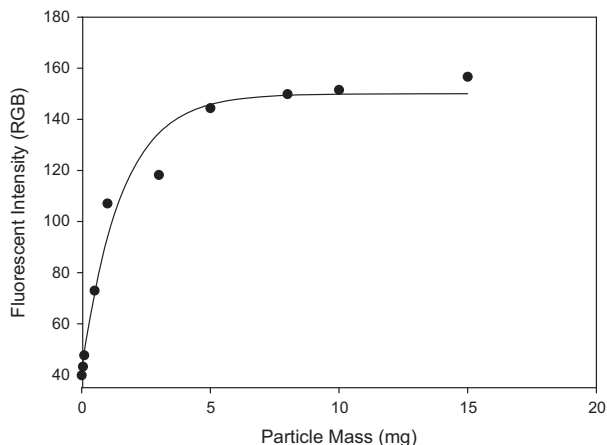


Fig. 3. Correlation of the particle mass and fluorescent intensity (particles made from 50% dilution were used and fluorescent intensity represented the RGB value obtained from image analysis).

3.2. Fluorescent decay of particles

One of the major problems when using fluorescent particles is the leakage of dye molecules from the silica fluorescent particles after being dispersed in aqueous solution. In the case of TMR-dextran-doped nano-particles, the hydrophilic properties of the dye allow serious leakage of the dye into the aqueous solutions where the fluorescence intensity decreases to 40% of the original values [19]. In this study, the dying process of the particles is carried out by incorporating the particles in a DMF solution where particles swell up to 2.5 times their dry volume [16]. While in this process, the dye molecules (RBITC) are doped inside the silica matrix [15]. And since the

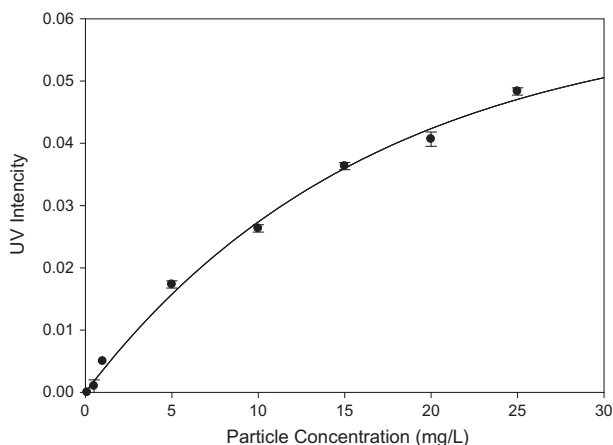


Fig. 4. Correlation of the particle concentration and UV intensity (particles made from 50% dilution were used and UV intensity represented the UV absorbance value obtained from the UV spectrometer).

Table 1
UV spectrometer detection limit

Concentration (mg/L)/ UV absorbance	0.1	0.5	1.0	5.0
#1	0	0.001	0.005	0.018
#2	0	0.002	0.005	0.017
#3	0	0	0.005	0.017

particles swell up as they are dispersed in an aqueous solution the dyeing agent would escape from the silica matrix. Thus, the synthesized particles should be tested to see whether the RBITC (dyeing agent) would leak in the aqueous solvents inducing the decreasing of fluorescence intensity. To evaluate the degree of dye leakage from the synthesized particles in an aqueous solution, the change of fluorescence intensity of particles was measured after being dispersed for 24 and 72 h in 100% ethanol solution. This experiment would present the maximum dye-leakage possible in an aqueous solution because the previous study showed the swelling of the particles was greater in ethanol than water [16]. UV spectrometer absorbance and RGB value from image analysis were used to evaluate the degree of fluorescence decay. Prior to each measurement, the particles were centrifuged and washed with ethanol to remove any free RBITC particles in the solution.

As result Fig. 5 shows, the UV absorbance changed (RBITC leaked out of the particles) within a range of 0–15% and an average of 3% decay as compared with

the original fluorescence within 24 h. However, particles submerged for 72 h in the aqueous solution showed fluorescence decay measuring from 10% to 44% lower than the initial value with the average of about 77% of the initial fluorescence absorbance. The RGB values obtained from the image analysis also indicate the fluorescence intensity decreased with time. After 72 h, the average RGB value became 40% lower than the initial value. From the result, it can be derived that the fluorescent intensity of particles is stable within 24 h of solvent submersion. This means that the fluorescent particles should be applied to the test within 24 h after the particle is dissolved into water. Otherwise, even though the particle has been utilized once in the test it can be reused within 24 h.

3.3. Effect of fluorescent particles on membrane fouling

Three different particles made from 1, 5, and 50% dilution (the size of particle for each dilution is presented in Table 2) were used in the experiment to assess the particle rejection rate and effect of fluorescent particles on the membrane fouling. The rejection rate of particles was measured by weighing the membranes before and after the filtration process: the weight of membranes filtered with particles was measured after dehydration in a desiccator for 24 h while three intact membranes filtered with ethanol and DI water were also weighed after dehydration to monitor for weight changes in the membranes alone. As a result, Fig. 6 shows the membrane rejection rate of particles with different sizes. The removal efficiency of particles with 50% dilution was up to 99%, while the particles with 1% and 5% dilution were rejected by about 85%. This result indicates that the membrane

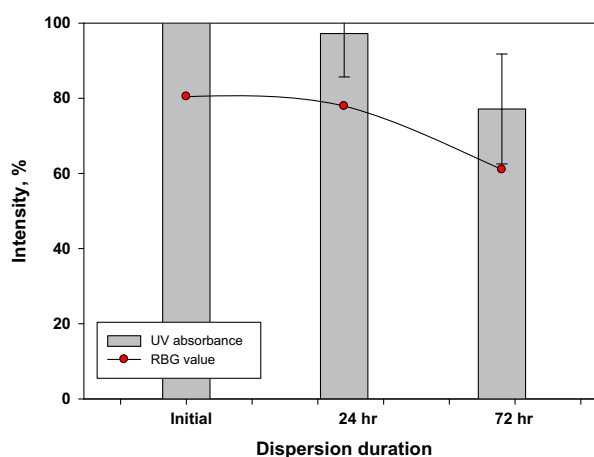


Fig. 5. Dye-leakage test of fluorescent particles dispersed in 100% ethanol solution.

Table 2
Size of particles in the feed solution and permeate after filtration

Dilution	Particle size in feed water (nm)		Particle size in permeate (nm)	
	Measurement	Ave. value (Std. deviation)	Measurement	Ave. value (Std. deviation)
1%	235	208 (25)	111	91 (17)
	203		79	
	187		84	
5%	158	161 (37)	63	69 (7)
	199		77	
	126		69	
50%	778	817 (36)	167	113 (48)
	848		93	
	825		77	

rejected not all of the particles. The particles with smaller size than the membrane pores would pass through the membrane. Therefore, to evaluate the size distribution of the particles that permeated through the membrane, a size analyzer (Zetasizer, Malvern) was used to measure the size of fluorescent particles retained in the feed and permeate solution. Table 2 presents the size distribution of particles measured for three different dilution factors in the feed and permeates. It is implied from the results that particles smaller than 167 nm mainly passed through the membrane, while the particles larger than 200 nm were rejected by membrane. This result is reasonable because the membrane used in the experiment has the nominal pore size of 0.25 μm (250 nm).

To evaluate the effects of the particles on membranes, a series of filtration tests were conducted to measure the membrane resistance, cake resistance, and internal pore adsorption resistance of the particles (Table 3). Before each test, the clean water flux of both

sides of the membrane was tested for the determination of the membrane resistance. Then the feed solutions including the particles with three different sizes were filtered through the membranes. The total resistance was calculated by using the resistance-in-series model ($J = P/\mu R$) with the consideration of the transmembrane pressure and flux at steady state. The resistance of internal pore adsorption was determined by overturning the tested membrane and measuring the flux decline when it was filtered with the clean water. The cake resistance was acquired by subtracting the internal pore and membrane resistance from the total resistance. As result Table 3 shows, the total resistance of a particle with 1% dilution was about 2 times higher than a particle with 50% dilution. As for the particle with 1% dilution, the cake layer and the internal pore resistance contributed 31% and 23% to the total resistance, respectively. Meanwhile, only a small portion of total resistance was attributed to the cake layer and internal pore resistance (9% and 7%, respectively) in the case of the particle with 50% dilution. It should be noted that as the dilution factor increased from 1 to 50% the size of particle also increased, while the contribution of cake layer and internal pore resistance to the total resistance decreased. This trend is very consistent with the fact that as the size of particle increases, the porosity of the cake layer also increases, resulting in the lower cake layer resistance. However, as particle size becomes smaller, the cake layer resistance increased as well as the internal pore resistance.

In summary, the particle with the size of 817 nm (50% dilution) showed almost no impact on the membrane fouling. When considering the pore size of the membrane used was 0.25 μm (250 nm), the particles with the pore size of about three times larger than the membrane pore were the most compatible as

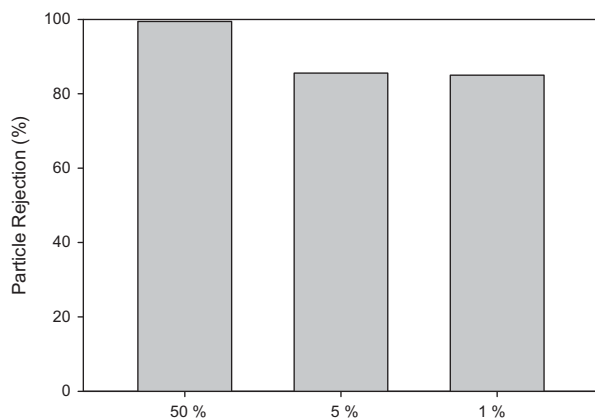


Fig. 6. Particle retention of membranes with different particles.

Table 3
Effects of fluorescent particles on the membrane fouling

Ave. particle size (dilution)	Total resistance		Membrane resistance		Cake layer resistance		Internal pore resistance	
	m^{-1} (10^{11})	%	m^{-1} (10^{11})	%	m^{-1} (10^{11})	%	m^{-1} (10^{11})	%
208 nm (1%)	2.25	100	1.06	47	0.69	31	5.10	23
161 nm (5%)	1.77	100	1.01	57	0.44	25	0.33	18
817 nm (50%)	1.18	100	0.99	84	0.11	9	0.08	7

surrogates for the integrity test to prevent the undesirable membrane fouling.

3.4. Particle outflow through damaged membranes

A series of experiments were conducted to evaluate the reliability of the integrity test by using the fluorescent particles as a surrogate. For this experiment, holes with different sizes (0.3, 0.5, and 1.0 mm in diameter) were punctured on a membrane surface artificially by using a syringe needle. The particle with 50% dilution (817 nm in average size) was used as a surrogate. The filtration test was performed for a punctured membrane with the feed solution containing the fluorescent particles of 30 mg/L by using the Amicon cell.

After filtration, image analysis was conducted on the collected permeate containing the fluorescent particles outflow from the breach of the membrane. Thus, the fluorescence intensity was represented by an RGB value on average. Then, the mass of outflow particles was estimated from the RGB value by referring to Fig. 3 which represented the functional relationship between the RGB value and the particle mass. Finally,

the rejection rate was calculated by dividing the predicted outflow particles mass by the total mass of particles in the feed solution. The total mass of particles in the feed was calculated simply by multiplying the particle concentration by the volume of feed solution. As a result, Fig. 7 represents that a punctured hole of 0.3 mm yielded 63% rejection rate, while holes of 0.5 and 1.0 mm showed 54.3% and 37.9% rejection rates, respectively. Additionally, Fig. 7 shows that the rejection rate decreased almost linearly with an increase in holes' diameter. This implies that as the breach of the membrane surface increased, the more fluorescent particles would pass through, thus resulting in the decrease in the particle rejection rate. Therefore, the size of breach on the membrane surface can be predicted possibly from the image analysis of the permeate containing the fluorescent particles outflow from a damaged part of membrane surface.

4. Summary

In this research, fluorescent particles were used as surrogate detectors to inspect the damaged part of an impaired membrane. Through the experiments, the following results could be concluded. (1) The image analysis was successfully performed to calculate the particle mass rejected on the membranes as well as the outflow mass in permeates. (2) Fluorescent particles with considerable sizes are suitable for integrity tests in which the effect of particles on membrane fouling is not significant. (3) The size of the membrane breach can be predicted as a function of the image analysis on the fluorescence intensity of the permeate containing the fluorescent particle's outflows. (4) Fluorescent particles used in the experiment can be retained in aqueous solutions for 24 h without compromising the fluorescent characteristics. As proven in the results above, the image analysis can be used as an appropriate method for integrity tests on damaged membranes. With continuous research, the results acquainted from this research may later lead to a more advanced analysis method with consideration of

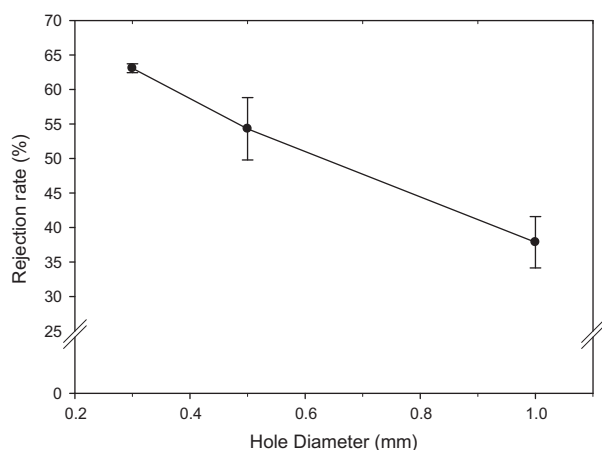


Fig. 7. Rejection rate of fluorescent particles from damaged membranes with different sizes of breaches, which was calculated by the image analysis (0.1, 0.5, and 1.0 mm in hole diameter on membrane surface).

various parameters that impact on the prediction and detection of the damaged part of membranes.

Acknowledgements

The authors would like to thank the Ministry of Environment for supporting this study through the Next-generation Core Environmental Technology Development Project (071-081-129) and also appreciate the support from the Ministry of Education, Science and Technology (MEST) (Grant No. NRF-2011-0029028 and NRF-2012R1A1A1006307).

References

- [1] U.S. EPA, Membrane Filtration Guidance Manual, EPA 915-d-03-008, U.S. Environmental Protection Agency Office of Water.
- [2] H. Guo, Y. Wyart, J. Perot, F. Nauleau, P. Moulin, Low-pressure membrane integrity tests for drinking water treatment: A review, *Water Res.* 44 (2010) 41–57.
- [3] K. Farahbakhsh, D.W. Smith, Estimating air diffusion contribution to pressure decay during membrane integrity tests, *J. Membr. Sci.* 237 (2004) 203–212.
- [4] S. Giglia, M. Krishnan, High sensitivity binary gas integrity test for membrane filters, *J. Membr. Sci.* 323 (2008) 60–66.
- [5] W.T. Johnson, Predicting log removal performances of membrane systems using in situ integrity testing, *Filtr. Sep.* 1 (35) (1998) 26–29.
- [6] S.S. Adham, J.G. Jacangelo, J.M. Laine, Low-pressure membrane: Assessing integrity, *J. AWWA* 3 (1995) 62–75.
- [7] U.S. EPA, Low-pressure membrane Filtration for Pathogen Removal: Application Implementation, and Regulatory Issues. EPA 815-c-01-001, U.S. Environmental Protection Agency Office of Water.
- [8] J. Deluhery, N. Rajagopalan, Use of paramagnetic particle in membrane integrity testing, *J. Membr. Sci.* 318 (2008) 176–181.
- [9] H. Guo, Y. Wyart, J. Perot, F. Nauleau, P. Moulin, Application of magnetic nanoparticles for UF membrane integrity monitoring at low-pressure operation, *J. Membr. Sci.* 350 (2010) 172–179.
- [10] V. Gitis, R.C. Haught, R.M. Clark, J. Gun, O. Lev, Application of nanoscale probes for the evaluation of the integrity of ultrafiltration membranes, *J. Membr. Sci.* 276 (2006) 185–192.
- [11] V. Gitis, R.C. Haught, R.M. Clark, J. Gun, O. Lev, Nanoscale probes for the evaluation of the integrity of ultrafiltration membranes, *J. Membr. Sci.* 276 (2006) 199–207.
- [12] V. Gits, A. Adin, A. Nasser, J. Gun, O. Lev, Fluorescent dye labeled bacteriophages—a new tracer for the investigation of viral transport in porous media: 1, *Intr. Charact. Water Res.* 36 (2002) 4227–4234.
- [13] P. Trimboli, J. Lozier, W. Johnson, Demonstrating the integrity of a large scale microfiltration plant using a bacillus spore challenge test, *Water Sci. Technol.* 1 (2001) 1–12.
- [14] W. Stöber, A. Fink, Controlled growth of monodisperse silica spheres in the micron size range, *J. Colloid Interface* 26 (1968) 62–69.
- [15] S.H. Choi, J.H. Yang, C.W. Suh, J.W. Cho, Use of fluorescent silica particles for checking the integrity of microfiltration membrane, *J. Membr. Sci.* 367 (2011) 306–313.
- [16] C.R. Miller, R. Vogel, P.P.T. Surawski, K.S. Jack, S.R. Corrie, M. Trau, Functionalized organosilica microspheres via a novel emulsion-based route, *Langmuir* 21 (2005) 9733–9740.
- [17] R. Vogel, P.P.T. Surawski, B.N. Littleton, C.R. Miller, G.A. Lawrie, B.J. Battersby, M. Trau, Fluorescent organosilica micro- and nanoparticles with controllable size, *J. Colloid Interface Sci.* 310 (2007) 144–150.
- [18] J. Ren, S. Song, A. Lopez-Valdivieso, J. Shen, S. Lu, Dispersion of silica fines in water–ethanol suspensions, *J. Colloid Interface Sci.* 238 (2001) 279–284.
- [19] X. Zhao, R.P. Bagwe, W. Tan, Development of organic-dyed silica nanoparticles in a reverse microemulsion, *Adv. Mater.* 16 (2004) 173–176.